Full-Duplex Dual-Band Radio Dedicated to Flexible Radio Communications

Zhaowu Zhan, Guillaume Villemaud, Florin Hutu, Jean-Marie Gorce

Full-Duplex Dual-Band Radio Dedicated to Flexible Radio Communications

Zhaowu Zhan, Guillaume Villemaud, Florin Hutu, Jean-Marie Gorce

RESEARCH REPORT

N° 8558

July 2014

Project-Teams SOCRATE

ISSN 0249-6399 ISRN INRIA/RR--8558--FR+ENG

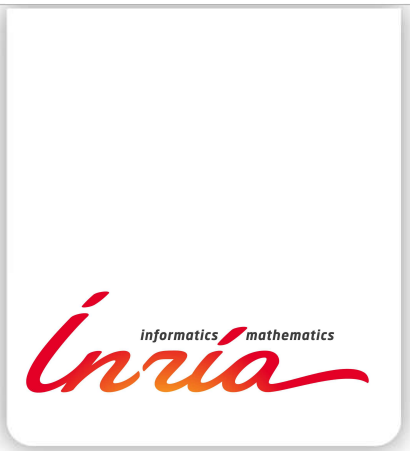

Full-Duplex Dual-Band Radio Dedicated to Flexible Radio Communications

Zhaowu Zhan*, Guillaume Villemaud*, Florin Hutu*,
Jean-Marie Gorce*

Project-Teams SOCRATE

Research Report n° 8558 — July 2014 — 12 pages

Abstract: This report presents the design of Full-Duplex Dual-Band radio which allows simultaneous transmission and reception in two separate spectrum fragments by combining the Full-Duplex radios and Dual-Band RF front-end. Our design employs two antennas, each one being used for simultaneous transmitting and receiving. To overcome the self-interference (SI) induced by the Full-Duplex radios, simple band pass filters (BPF) are utilized to suppress the inner SI and active analog self-interference cancellation (AASIC) method is used to cancel the inter SI. The two radio frequency (RF) signals corrupted individually by the residual SI are down-converted by the double I/Q structure. Then, the two output baseband signals are processed by the corresponding baseband receivers. We theoretically analyze and evaluate by simulation this Full-Duplex Dual-Band radio operating on the standard WiFi OFDM PHY in two separate spectrum fragments.

Key-words: Full-Duplex wireless, Dual-Band radio, flxible radio communications

* Université de Lyon, INRIA, INSA-Lyon, CITI-INRIA, F-69621, Villeurbanne, France

RESEARCH CENTRE
GRENOBLE – RHÔNE-ALPES

Inovallée
655 avenue de l'Europe Montbonnot
38334 Saint Ismier Cedex

Radio Full-Duplex Dual-Band Dédié à Communications Radio Flexibles

Résumé : Ce rapport présente le design d'un système radio Full-Duplex dual-band qui permet la transmission et la réception en simultanées de deux fragments de spectre séparés en combinant l'approche Full-Duplex à un frontal RF dual-bande. Notre structure requière deux antennes, chacune étant utilisée pour l'émission et la réception simultanément. Pour résoudre le problème d'auto-interférence (SI) induit par le Full-Duplex, de simples filtres passe-bande (BPF) sont utilisés pour supprimer l'auto-interférence interne et une suppression active de l'auto-interférence au niveau analogique (AASIC) est ajoutée pour supprimer l'auto-interférence croisée. Les deux signaux RF brouillés par l'auto-interférence résiduelle sont transposés en bande de base pour une structure à double IQ. Alors, chaque signal obtenu en bande de base est démodulé par le récepteur approprié. Nous présentons ici une analyse théorique et une évaluation en simulation de cette architecture Full-Duplex Dula-Band fonctionnant sur le standard WiFi OFDM dans deux bandes séparées.

Mots-clés : radio Full-Duplex, radio bi-bande, communications radio flexibles

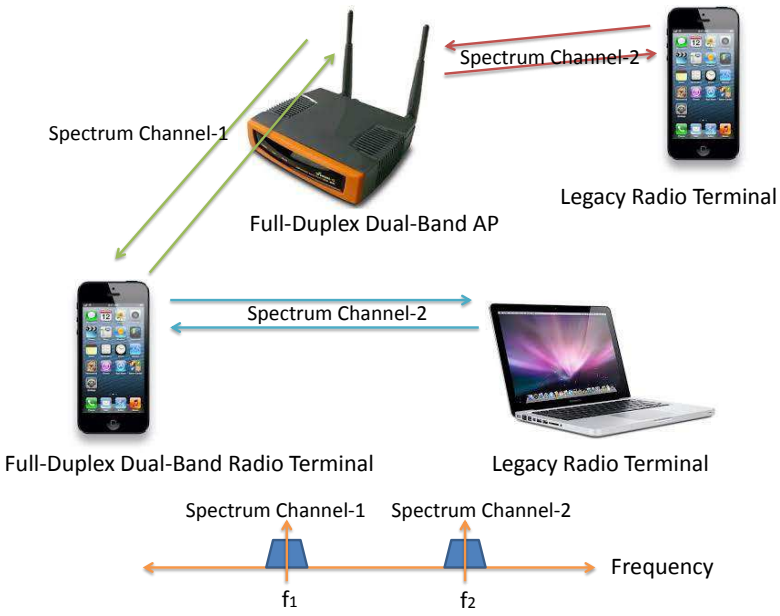

Figure 1: The second self-interference cancellation model

1 Introduction

Full-Duplex is defined as a radio which can simultaneously transmit and receive in the same frequency band [1] [2]. Dual-Band radio can simultaneously process two different kind of signals, even different physical layer signals, by using one common radio frequency (RF) front-end, for instance with a double I/Q structure [3]. Full-Duplex Dual-Band radio based on the combination of Full-Duplex radio and Dual-Band radio enable the radio node to transmit and receive simultaneously on each separate spectrum fragment with one common RF front-end.

Many applications can benefit from the capability of simultaneously transmit and receive on each separate spectrum fragment with one common RF front-end. By this capability, the radio terminal can simultaneously transmit, simultaneously receive or simultaneously transmit and receive on both of the two separate spectrum fragments. For instance, one Full-Duplex Dual-Band radio terminal can communicate simultaneously with two radio terminals as shown in Fig. 1. With respect to the Full-Duplex Dual-Band AP (Access Point: Femto Base Station or WiFi Router), it can accommodate two different clients simultaneously on two different spectrum channels operating on in-band Full-Duplex model. That means the Full-Duplex Dual-Band radio enhance the capacity of an AP by four times compared to the conventional AP which is restricted to the use of only one channel at a time operating on Half-Duplex model. Similarly, the radio terminal such as a mobile phone equipped with the Full-Duplex Dual-Band radio can communicate with the Femto base-station for voice transmission and reception while connecting with laptop for media or files downloading and uploading. Therefore, Full-Duplex Dual-Band radio could provide the users much more flexible radio connection and higher aggregate throughput than the current radio terminals operating on Half-Duplex model in a single spectrum channel at a time.

Such a capability could also be exploited to enhance the radio sharing and coexistence. Portable radio terminals such as smartphones have to accommodate a growing list of wireless standards such as WiFi, Zigbee, Bluetooth, 3G and 4G. Current practical implementation is

to use separate radio and antenna to meet the different standard requirement, which is costive and also put high requirements on the space of portable consumer devices. Instead, Full-Duplex Dual-Band radio could enable the radio terminal to accommodate two different wireless standards with one common RF front-end.

In this report, we first studied and demonstrated the Full-Duplex Dual-Band radio via operating on the standard WiFi OFDM PHY in two separate spectrum fragments. The studied radio architecture can be used to enhance the current WiFi system but it is not just limited to that. For example, the radio can operate on the two standards of WiFi and UMTS, WiFi and Zigbee, or 3G and WiFi, and so on.

The rest of the report is organized as follows: Section 2 presents the details of the proposed Full-Duplex Dual-Band OFDM radio transceiver, including Full-Duplex radios and Dual-Band RF front-end. In Section 3, we calculate the power of residual SI to qualify the impact of residual SI caused by Full-Duplex radio on the proposed radio system. Then, the simulation results and discussion are given in Section 4. Finally, the conclusion is drawn in Section 5.

2 Full-Duplex Dual-Band Radio Transceiver

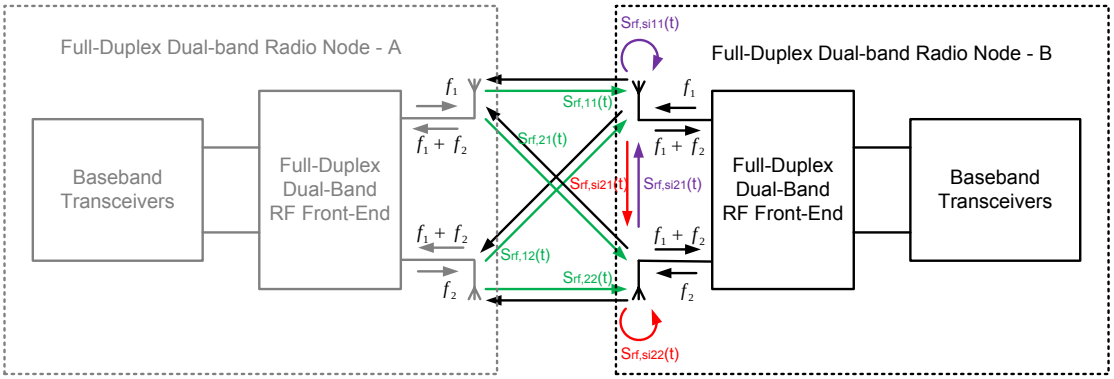

Figure 2: Block diagram of the Full-Duplex Dual-Band wireless radios

In this Section, we first present the general block diagram of the Full-Duplex Dual-Band radio system as shown in Fig. 2 and then the details of the radio transceiver as shown in Fig. 3. As we can see, this radio node employs two antennas which are compatible with future multi-antenna systems. Each antenna is used for simultaneous transmission and reception via a circulator [4] [5] separating the input and output signals, which builds the one-antenna Full-Duplex. From the perspective of both of the two antennas, they are utilized for simultaneously transmitting and receiving, which builds the two-antenna Full-Duplex. Therefore, each antenna of the radio node-B (local radio node) will not only receive the RF signals from the radio node-A (distant radio node) but also the RF SI signal from its own transmission. Then, the signals received by the i^{th} antenna of the local radio node plus the SI signal leaked from the circulator can be represented by

$$S_{rf,i}(t) = S_{rf,ij}(t) + S_{rf,ii}(t) + S_{rf,si_{ij}}(t) + aS_{rf,si_{ii}}(t), \{i,j\} \in A \quad (1)$$

where $S_{rf,ij}(t)$ and $S_{rf,ii}(t)$ are the RF signals emitted by the j^{th} antenna and i^{th} antenna of the distant radio node respectively and received by the i^{th} antenna of the local radio node, $S_{rf,si_{ij}}$

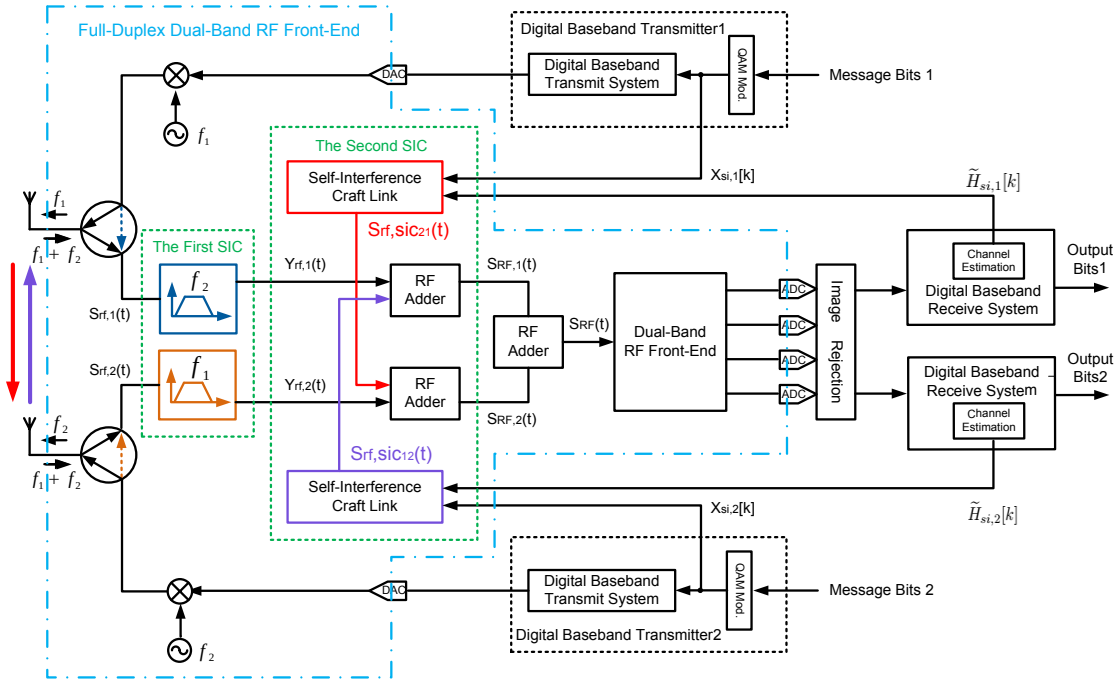

Figure 3: Full-Duplex Dual-Band radio transceiver

denotes the inter RF SI signal transmitted from the j^{th} antenna and received by the i^{th} antenna of the local radio node, $S_{rf,si_{ii}}$ is the inner RF SI signal transmitted and received by the same antenna and circulator, a being the inner-SI factor including multi-path reflection factor and inner leakage factor of the circulator and $A \triangleq \{i \in [1,2], j \in [1,2], i+j=3\}$.

2.1 Full-Duplex Radios

Although the Full-Duplex can improve spectral efficiency and also provide the benefits beyond radio link capacity, it brings to the proposed radio system a strong SI which could saturate the radio receivers. From (1), it can be seen that the receptions of the desired signals from the distant radio node are challenged by the strong inner SI caused by the one-antenna Full-Duplex and inter SI induced by the two-antenna Full-Duplex. These SIs could be hundreds of thousands times of the desired signal. Therefore, suppressing or reducing the strength of the SI signal to a tolerable level is the key point for designing a real Full-Duplex Dual-Band radio. In the proposed radio transceiver, the SI includes inner SI and inter SI. In order to mitigate these two types of SI, we implement two self-interference cancellations (SIC) as shown in Fig. 3. For suppressing the inner SI, we utilize normal BPFs to build the first SIC. While with respect to inter SI, the active analog SIC (AASIC) method [6] is used to implement the second SIC.

2.1.1 The First Self-Interference Cancellation

The first SIC is to carry out the suppression of inner SI induced by the one-antenna Full-Duplex. In fact, the inner SI $aS_{rf,si_{ii}}$ includes the reflection-path SI transmitted and received by the same

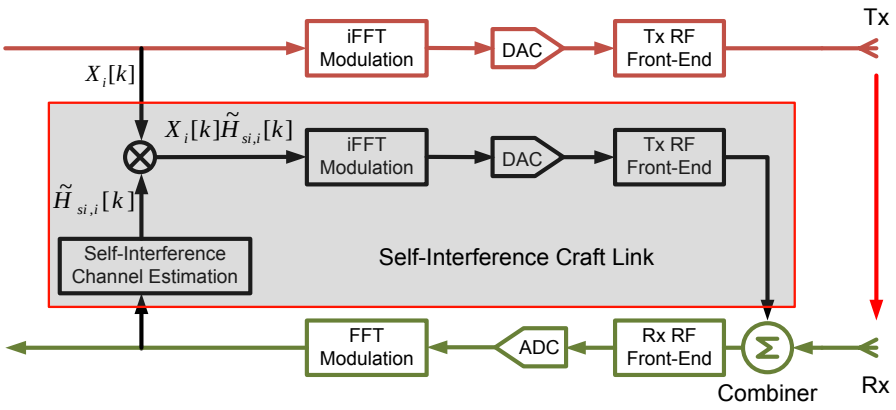

Figure 4: The second self-interference cancellation model

antenna and the SI leaked from the imperfect circulator. BPF-i (perfect BPF is assumed) with center frequency f_j is used here to implement the first SIC which eliminates the inner SI signal $aS_{rf,si_{ii}}(t)$ and also filters out the distant radio signal $S_{rf,ii}(t)$ with carrier frequency f_i. That means the first SIC eliminates completely the SI caused by the one-antenna Full-Duplex. Then, the RF signals with carrier frequency f_j including signal of interest $S_{rf,ij}(t)$ and the over-the-air SI signal $S_{rf,si_{ij}}(t)$ can be represented by

$$Y_{rf,i}(t) = S_{rf,ij}(t) + S_{rf,si_{ij}}(t), \{i,j\} \in A \tag{2}$$

2.1.2 The Second Self-Interference Cancellation

After eliminating the inner SI, the inter SI induced by the two-antenna Full-Duplex is still strong enough to saturate the radio receiver. In order to cancel the inter SI signal $S_{rf,si_{ij}}(t)$ in (2), [2] [7] proposed active SI cancellation (ASIC) and [8] focus on passive SI suppression (PSIS). As it has been introduced in Section I, we first study the Full-Duplex Dual-Band radio operating on the standard WiFi OFDM PHY. Therefore, we can simplify the two-antenna Full-Duplex model and SIC model as shown in Fig. 4. We craft the RF cancellation signal in another radio link as presented in [6] and implement the SIC at the RF stage. Then, the SIC model used in this report can be expressed as

$$\begin{aligned} r_{RF,rsi,j}(t) \quad = \quad & \sqrt{P_{si}}\sqrt{L_{si}}\mathsf{IDFT}\left\{X_i[k]\right\} e^{j2\pi f_i t} * h_{si,i}(t) \\ & -\sqrt{P'_{si}}\sqrt{L'_{si}}\mathsf{IDFT}\left\{X_i[k]\widetilde{H}_{si,i}[k]\right\} e^{j2\pi f_i t} \end{aligned} \tag{3}$$

where $r_{RF,rsi,j}(t)$ denotes the received residual RF SI, from the i^{th} antenna of the local radio node, in the j^{th} receiver chain, P_{si} and P'_{si} represent the transmit power of the transmitter and the cancellation link respectively, L_{si} and L'_{si} denote the path loss of the SI channel and the cancellation link respectively, $X_i[k]$ is the symbol to be transmitted from the i^{th} antenna, $h_{si,i}(t)$ denotes the impulse response of the wireless SI channel from the i^{th} antenna to the j^{th} antenna, $\widetilde{H}_{si,i}[k]$ represents the estimated coefficients in the frequency domain of the $h_{si,i}(t)$, f_i denotes the carrier frequency of the i^{th} transmitter chain and $*$ represents time domain convolution. $\mathsf{IDFT}\{\chi_m[k]\} \triangleq \frac{1}{T_u}\sum_{k=-\frac{N}{2}}^{\frac{N}{2}} \chi_m[k]e^{j2\pi\Delta fkt}$, in which T_u is the duration of one OFDM symbol, N denotes the total number of sub-carriers and Δf denotes the sub-carrier space.

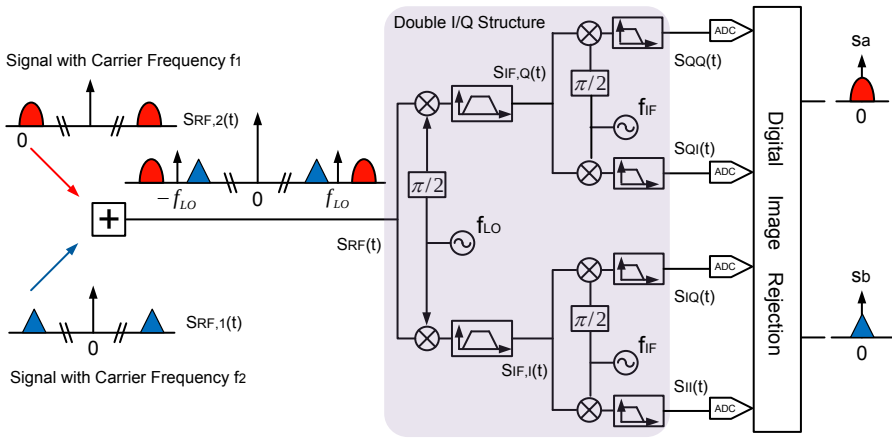

Figure 5: Architecture of Dual-Band RF front-end

After the second SIC, the remaining received signal in the i^{th} receiver chain can be expressed as

$$S_{RF,i}(t) \quad = \quad S_{rf,ij}(t) + r_{RF,rsi,i}(t) \tag{4}$$

Therefore, the RF signal $S_{RF,i}(t)$ to be input to the Dual-Band radio consists of the desired signal from the distant radio node and the residual inter SI which can be regarded as another receiver noise superposed on the desired signal. Taking the received RF signal $S_{RF,1}(t)$ in the 1^{st} receiver chain as an example, this RF signal includes the desired signal $S_{rf,12}(t)$ with carrier frequency f_2 from the 2^{nd} antenna of distant radio node and the residual SI $r_{RF,rsi,1}(t)$ with the same carrier frequency as $S_{rf,12}(t)$. In order to qualify the impact of the residual SI on the reception of the signal of interest, we will calculate the power of the residual SI in Section III.

2.2 Dual-Band RF Front-End

After the two SICs mitigating the SI induced by the Full-Duplex radios, the two received useful RF signals superposed by the residual SI will be down-converted to baseband signal by using Dual-Band radio with double I/Q structure. The received RF signal $S_{RF,i}(t)$ is with carrier frequency f_j, so we define $S'_{RF,1}(t) \triangleq S_{RF,2}(t)$ and $S'_{RF,2}(t) \triangleq S_{RF,1}(t)$. Then, the Dual-Band RF front-end is used to separate the RF signals $S'_{RF,1}(t)$ with carrier frequency f_1 and $S'_{RF,2}(t)$ with carrier frequency f_2. In order to facilitate the theoretical study of the Dual-Band RF front-end, we use $s_i = I_i + \jmath Q_i, \{i \in [1,2], \jmath^2 = -1\}$ denote the equivalent baseband complex symbols carried by the frequency f_i . Then, the received RF signal-1 $S'_{RF,1}(t)$ and RF signal-2 $S'_{RF,2}(t)$ can be expressed as

$$\begin{aligned} S'_{RF,1}(t) &= I_1(t)cos(2\pi f_1 t) - Q_1(t)sin(2\pi f_1 t) \\ S'_{RF,2}(t) &= I_2(t)cos(2\pi f_2 t) - Q_2(t)sin(2\pi f_2 t) \end{aligned} \tag{5}$$

Note that the signal model in (5) is reasonably valid even in a noisy environment, because $I_i(t)$ can represent the sum of the real part of the data symbol and noise (including receiver thermal noise and residual SI) and $Q_i(t)$ can represent the sum of the image part of the data symbol and noise (including receiver thermal noise and residual SI) respectively.

As shown in Fig. 5, after the received RF signal $S_{RF}(t) = S'_{RF,1}(t) + S'_{RF,2}(t)$ going through the first frequency translation stage with carrier frequency $f_{LO} = \frac{f_1+f_2}{2}$, and the pass band signals are filtered out. Then, the I/Q branch of intermediate frequency (IF) signals can be obtained as

$$S_{IF,I}(t) = \frac{I_1(t) + I_2(t)}{2} cos(2\pi f_{IF} t) + \frac{-Q_1(t) + Q_2(t)}{2} sin(2\pi f_{IF} t) \quad (6)$$

$$S_{IF,Q}(t) = \frac{I_1(t) - I_2(t)}{2} sin(2\pi f_{IF} t) + \frac{Q_1(t) + Q_2(t)}{2} cos(2\pi f_{IF} t) \quad (7)$$

where $f_{IF} = \frac{f_1-f_2}{2} = f_1 - f_{LO} = f_{LO} - f_2$.

The baseband signals $s_{II}(t)$, $s_{IQ}(t)$, $s_{QI}(t)$ and $s_{QQ}(t)$ obtained by down-converting IF signals $S_{IF,I}(t)$ and $S_{IF,Q}(t)$ with frequency f_{IF} can be expressed as

$$\begin{aligned} s_{II}(t) &= \frac{I_1(t) + I_2(t)}{4}; \\ s_{IQ}(t) &= \frac{Q_1(t) - Q_2(t)}{4}; \\ s_{QI}(t) &= \frac{Q_1(t) + Q_2(t)}{4}; \\ s_{QQ}(t) &= \frac{-I_1(t) + I_2(t)}{4}. \end{aligned} \quad (8)$$

After the analog-to-digital converter (ADC) and digital-image-rejection, the received baseband complex symbols s_a and s_b corresponding to the symbols s_1 and s_2 which include the baseband symbols from the distant radio node are given by

$$s_a = (s_{II} - s_{QQ}) + \jmath(s_{QI} + s_{IQ}) = \frac{s_1}{2} \quad (9)$$

$$s_b = (s_{II} + s_{QQ}) + \jmath(s_{QI} - s_{IQ}) = \frac{s_2}{2} \quad (10)$$

Therefore, the two RF signals $S'_{RF,1}(t)$ and $S'_{RF,2}(t)$ are down-converted and separated completely by using the Dual-Band RF front-end.

From the above studies, it can be seen that the Full-Duplex Dual-Band radio could down-convert and separate two different types of RF signals which are in two separate spectrum fragments. The two output baseband symbols s_a and s_b including the baseband symbols from the distant radio node and additive noise (receiver thermal noise and residual SI) are further processed by the corresponding baseband receivers.

3 Residual Self-Interference

In the report, the proposed Full-Duplex Dual-Band radio operates on the standard baseband WiFi OFDM PHY. Therefore, the available AASIC [6] method which is suitable for the OFDM SIC is used to cancel the inter SI induced by the two-antenna Full-Duplex as shown in Fig. 4. The radio node knows the transmit symbols $X_i[k]$ with $E\{|X_i[k]|^2\} = 1$, so it can implement the SIC as described in (3) if it can obtain the channel state information (CSI) of the over-the-air SI channel. In the standard WiFi, the long training sequence consisting of two known OFDM symbols in the preamble is used for channel estimation. In order to avoid the impact of the signal from the distant radio node on the SI channel estimation, we redesign the data frame in order that the long training symbols from different radio nodes take different time slots.

Perfect frequency and timing synchronization and no RF impairment are assumed. Therefore, at the receiver side, after the down-conversion of the RF signal received and removal of the cyclic prefix, the baseband frequency domain signal can be obtained by FFT of the time domain baseband signal. During the time of SI channel estimation, each radio node just receives the signal it transmits. The demodulated long training OFDM symbol in the i^{th} receiver chain can be expressed as:

$$R_{si,i}[k] = \sqrt{P_{si}}\sqrt{L_{si}}T_j[k]H_{si,j}[k] + Z[k], \{i,j\} \in A \tag{11}$$

where $T_j[k], k \in [1, N_{nz}]$ with $E\{|T_j[k]|^2\} = 1$ denotes the known BPSK symbol sequences, $H_{si,j}[k]$ is the SI channel from the j^{th} antenna to the i^{th} antenna and $Z_m[k]$ represents the frequency domain receiver thermal noise following the normal distribution $\mathcal{N}(0, \delta_n^2)$.

The CSI of the SI channel is estimated via dividing the demodulated long training symbols received by the pilot pattern with the known BPSK symbol sequences. Therefore, the estimated channel transfer function after normalization is

$$\begin{aligned} \widetilde{H}_{si,j}[k] &= \frac{R_{si,i}[k]}{\sqrt{P_{si}}\sqrt{L_{si}}T_j[k]} \\ &= H_{si,j}[k] + Z_m[k]/(\sqrt{P_{si}}\sqrt{L_{si}}T_j[k]) \end{aligned} \tag{12}$$

The second term of the right side of the (12) is the channel estimation error of the k^{th} subcarrier channel due to the receiver thermal noise.

With the estimated CSI of the SI channel available, the SIC is carried out as (3). After the interference cancellation, the residual baseband SI signal $r_{BB,rsi,j}(t)$ can be represented by (13) when the mixers in the RF front-end are perfect.

$$\begin{aligned} r_{BB,rsi,j}(t) &= \sqrt{P_{si}}\sqrt{L_{si}}\mathsf{IDFT}\left\{X_i[k]\right\} * h_{si,i}(t) - \sqrt{P'_{si}}\sqrt{L'_{si}}\mathsf{IDFT}\left\{X_i[k]\widetilde{H}_{si,i}[k]\right\} \\ &= \mathsf{IDFT}\left\{\sqrt{P_{si}}\sqrt{L_{si}}X_i[k]H_{si,i}[k]\right\} - \mathsf{IDFT}\left\{\sqrt{P'_{si}}\sqrt{L'_{si}}X_i[k]\widetilde{H}_{si,i}[k]\right\} \end{aligned} \tag{13}$$

According to the Parseval's theorem [9], the power of the time domain signal can be calculated in the frequency domain. The frequency domain residual SI can be represented by

$$R_{BB,rsi,j}[k] = \sqrt{P_{si}}\sqrt{L_{si}}X_i[k]H_{si,i}[k] - \sqrt{P'_{si}}\sqrt{L'_{si}}X_i[k]\widetilde{H}_{si,i}[k] \tag{14}$$

When $\sqrt{L_{si}}\sqrt{P_{si}} = \sqrt{L'_{si}}\sqrt{P'_{si}}$ and after replacing the $\widetilde{H}_{si,i}[k]$ in (14) by (12), the residual SI can be expressed as

$$R_{BB,rsi,j}[k] = -\frac{X_i[k]}{T_i[k]}Z'_m[k] \tag{15}$$

Because of the independence between $X_i[k]$ and $T_i[k]$ in (15), the power of the residual SI in the j^{th} receiver chain is

$$P_{rsi,j} = E[R_{BB,rsi,j}[k] \cdot R^*_{BB,rsi,j}[k]] = \delta_n^2 \tag{16}$$

That means we can reduce the SI to noise level and the residual SI could be regarded as another receiver thermal noise.

4 Simulation Results and Discussion

4.1 Simulation Results

In this report, we take the Full-Duplex Dual-Band radio operating on WiFi OFDM PHY in two separate spectrum fragments as the first study case. The two over-the-air SI channels are

assumed as single path one delay channel which rely on the fact that the strength of the direct path dominates the power of the SI channel [8].

The system parameters are chosen as in Table 1 according to the IEEE 802.11g WLAN standard.

Table 1: System Parameters

Parameter	Value
Bandwidth	20MHz
Carrier frequency f_1	2.4GHz
Carrier frequency f_2	2.0GHz
Total number of subcarriers	52
Number of data subcarriers	48
Number of pilot subcarriers	4
Bit rate	36Mbps
IFFT/FFT period	3.2us
GI duration	0.8us

We evaluate and demonstrate the Full-Duplex Dual-Band based radio system by employing the co-simulation of ADS (Advanced Design System, Agilent Tech.) and Matlab. The RF front-end and most of the baseband processing system are modeled by ADS and part of the digital signal processing are carried out by Matlab.

The Bit Error Rate (BER) is used to evaluate and compare the performance of IEEE 802.11g, Dual-Band IEEE 802.11g and Full-Duplex Dual-Band IEEE 802.11g as shown in Fig. 6. The BER curves of Dual-Band WiFi-1 and WiFi-2 overlap with that of conventional WiFi system when the Dual-Band RF front-end is ideal, i.e. without any RF impairment, which can be explained and demonstrated by Section II B. While with respect to the Full-Duplex Dual-Band WiFi system, there is around 3 dB gap to the conventional WiFi system. This 3 dB gap in each of the two radio branches is caused by the residual SI due to the thermal noise as presented in Section III. This implies that the proposed radio could simultaneously receive two different signals in two separate spectrum fragment at the cost of tolerable SINR loss. When the radio operating on the standard WiFi OFDM PHY, the SINR loss is just 3 dB.

4.2 Discussion

Full-Duplex is defined as a radio which can simultaneously transmit and receive in the same frequency band, which capability can enable the radio terminal to carry out spectrum channel sensing while working [10]. Dual-Band RF front-end enable the radio systems to simultaneously process two different types of signals. Such a capacity could provide the radio terminal a candidate spectrum channel for immediate channel handover. Therefore, the potential capability of carrying out the spectrum channel sensing and handover could render the proposed Full-Duplex Dual-Band radio a viable candidate radio technique for the cognitive radios.

5 Conclusion

Spectrum fragmentation will be compounded in 5G driven by the scarcity of spectrum [11], which requires flexible radio transceiver to support flexible utilization of spectrum fragment in the future wireless network. In this report, a flexible radio: Full-Duplex Dual-Band radio was

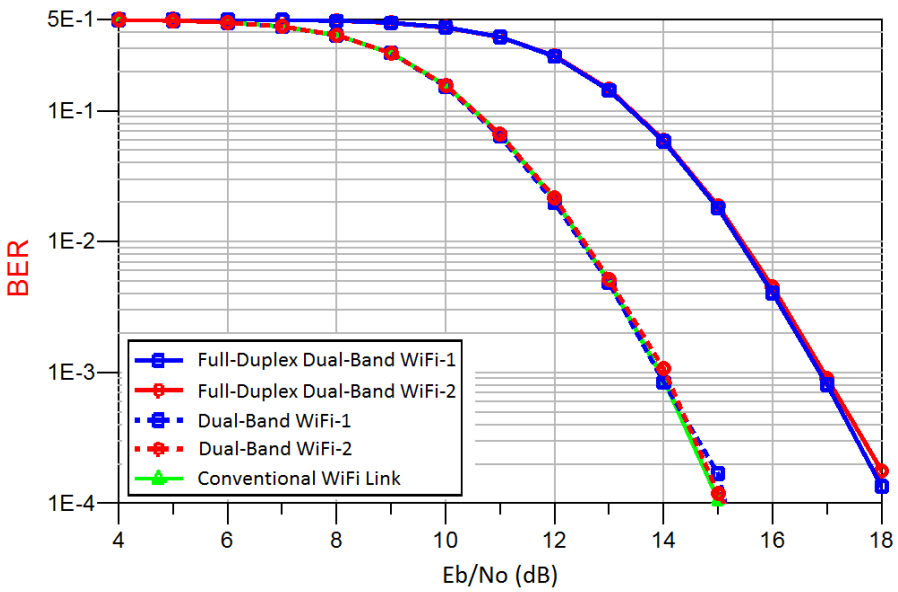

Figure 6: The BER of different radio transceiver with different Eb/No

proposed and studied via operating on the standard WiFi OFDM PHY. The proposed radio could simultaneously work on two separate spectrum fragments. In each spectrum fragment, this radio could enable the radio terminal to simultaneously transmit and receive. Such capabilities render it a seducing flexible radio system.

References

[1] M. Duarte, and A. Sabharwal, "Full-Duplex Wireless Communications using Off-the-Shelf Radios: Feasibility and First Results," in *IEEE Asilomar Conference on Signals, Systems and Computers*, 2009.

[2] M. Jain, J. Choi, T. Kim, D. Bharadia, K. Srinivasan, P. Levis, S. Katti, P. Sinha, S. Seth, "Practical Real-Time Full Duplex Wireless," in *ACM MOBICOM*, 2011.

[3] I. Burciu, G. Villemaud, J. Verdier and M. Gautier, "Low Power Front-End Architecture dedicated to the Multistandard Simultaneous Reception," *Cambridge International Jurnal of Microwaves and Wireless Technologies*, vol.2, no.6, pp 505-514, December 2010.

[4] D. Bharadia, E. McMilin and S. Katti, "Full Duplex Radios," in *ACM SIGCOMM*, 2013.

[5] S.S. Hong, J. Mehlman and S. Katti, "Picasso: flexible RF and spectrum slicing," in *ACM SIGCOMM*, 2012.

[6] Zhaowu Zhan, Guillaume Villemaud and Jean-Marie Gorce, "Design and Evaluation of a Wideband Full-Duplex OFDM System Based on AASIC," in *IEEE 24th International Symposium on Personal Indoor and Mobile Radio Communications*, 2013.

[7] M. Duarte, C. Dick, and A. Sabharwal, "Experiment Driven Characterization of Full-Duplex Wireless Communications," *IEEE Trans. Information Theory*, vol.11, no.12, pp. 4296-4307, Dec. 2012.

[8] Evan Everett, Achaleshwar Sahai, and Ashutosh Sabharwal, "Passive Self-Interference Suppression for Full-Duplex Infrastructure Nodes," *IEEE Transactions on Wireless Communications*, vol. 13, no. 2, pp. 680-694, February 2014.

[9] Z. Glenn and J. Fred, *Advanced Digital Signal Processing: Theory and Applications*, New York, USA: Marcel Dekker, INC, 1994.

[10] Y.S. Choi, Hooman. Shiranni-Mehr, "Simultaneous Transmission and Reception: Algorithm, Design and System Level Performance," *IEEE Transactions on Wireless Communications*, vol. 12, no. 12, pp. 5992-6010, December 2013.

[11] S. Hong, J. Brand, J. Choi, M. Jain, J. Mehlman, S. Katti and P. Levis, "Applications of Self-Interference Cancellation in 5G and Beyond," *IEEE Communications Magazine*, vol. 52, no. 2, pp. 114-121, February 2014.

Contents

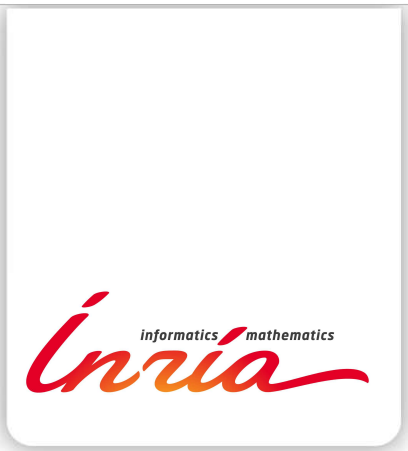

RESEARCH CENTRE
GRENOBLE – RHÔNE-ALPES

Inovallée
655 avenue de l'Europe Montbonnot
38334 Saint Ismier Cedex

Publisher
Inria
Domaine de Voluceau - Rocquencourt
BP 105 - 78153 Le Chesnay Cedex
inria.fr

ISSN 0249-6399